

# Durability Characterization of Low Ice Adhesion and Impact Resistance Coatings

Miranda L. Beaudry<sup>1</sup>, Christopher J. Wohl<sup>2</sup>, and Joseph G. Smith Jr<sup>2</sup>

<sup>1</sup>NASA Internship, Fellowship, and Scholarship Program, NASA Langley Research Center, Hampton, VA, 23681, USA

<sup>2</sup>NASA Langley Research Center, Hampton, VA, 23681, USA

[c.j.wohl@nasa.gov](mailto:c.j.wohl@nasa.gov)

## Introduction

Glaze, rime and mixed icing conditions can cause significant variation in aerodynamic performance, fuel efficiency, and flight safety. For commercial aircraft, active icing mitigation strategies are utilized to enable safe flight within icing conditions according to the FAR Part 25/29 Appendix C icing envelope.<sup>1</sup> For general aviation and unmanned aerial vehicles that cannot support active anti-icing technologies, avoidance is the only recourse. Passive approaches have been investigated to reduce weight and energy consumption for active systems and to expand the operational envelope for smaller aircraft.<sup>2</sup> Coatings are one passive method to reduce or mitigate ice accretion on frontal surfaces of commercial aircraft with the greatest region of interest being wing leading edges.<sup>3</sup>

Aircraft wing leading edges represent an extreme environment. Durability must be considered for any material to be applied as a coating in this area. Currently, there are no specifications regarding coating durability of a low ice adhesion material applied on the wing leading edge. Therefore, a reasonable starting point is to use the durability specifications put forth for an aircraft external coating.<sup>4</sup> Besides the tests called out in these specifications, others were included such as Taber abrasion to simulate wear and erosion.

Beyond durability, performance metrics with regards to adhesion strength of accreted in-flight (i.e., impact) icing are central to determine coating usefulness. Determination of this property though is particularly challenging and only a few facilities have the capability to quantify this.<sup>5</sup> An instrument at NASA Langley Research Center [Adverse Environment Rotary Test Stand Jr., (AERTS Jr.)], based on the AERTS system at The Pennsylvania State University,<sup>6</sup> allows for screening numerous coatings subjected to the icing environment.

To establish a benchmark for comparison with research coatings, a state-of-the-art (SOA) commercial aircraft coating was subjected to an array of salient durability and performance experiments. The same tests were conducted using a baseline epoxy (BE) resin formulation that demonstrated some initial promising results for comparison. Results from this initial screening will be discussed herein.

## Experimental

**Coating Preparation.** Coatings were fabricated on prepared aluminum (Al) substrates of Al 3003 for Taber abrasion, Al 2024 for impact testing, and Al 6061 for ice adhesion testing. Surfaces were prepared by 1) abrasion using a solution

of Pace<sup>®</sup> B-82 (Chemetall<sup>®</sup>), diluted in water by a factor of 7, until a water break-free surface was observed followed by 2) a solution of AC-131 (3M<sup>™</sup>) that had been mixed and agitated for at least 30 min before surface application.

The BE resin was prepared from the diglycidyl ether of bisphenol A (DGEBA, DER<sup>™</sup> 331, Dow<sup>®</sup> Chemical), a glycidyl ether-terminated poly(ethylene glycol) (PEG, Aldrich, number average molecular weight ~ 500 g/mol), and 1,3-bis(4-aminophenoxy)benzene at a hardener/epoxy ratio of 0.8. The PEG epoxy loading was 35 wt%. Once combined in a glass container, the mixture was heated in an oil bath at 90°C with stirring for a minimum of 45 min then cooled to room temperature (RT). It was then applied to prepared substrates by dispensing from a plastic syringe.

The SOA commercial coating was prepared according to manufacturer recommendations and applied to substrates prepared as described previously. The coating consisted of an epoxy primer and proprietary topcoat with nominal wet-thickness values for each layer (13 and 64  $\mu\text{m}$ , respectively). Specimens were cured at RT for a minimum of 14 days. Digital images of both coatings are shown in Fig. 1.

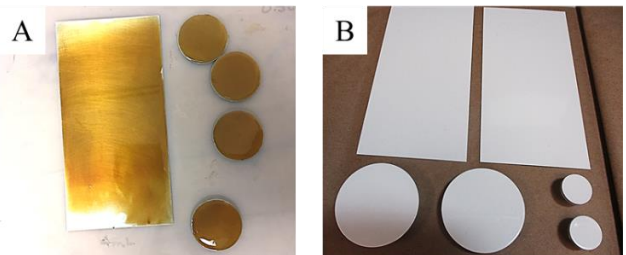


Figure 1. A) BE and B) SOA coated specimens.

**Physical Characterization.** Advancing and receding water contact angles ( $\theta_A$  and  $\theta_R$ , respectively) were determined on a First Ten Angstroms FTA1000B Goniometer (Gon) according to ASTM D7334 using water and ethylene glycol (EG). A minimum of 3 droplets were utilized for each surface. Interfacial tension measurements were conducted prior to testing to verify solvent purity and image resolution. Surface roughness was measured before impact icing using a Bruker Dektak XT Stylus Profilometer (Sty Prof). Measurements were conducted using a 12.5  $\mu\text{m}$  tip at a vertical range of 65.5  $\mu\text{m}$  with an applied force of 3 mg. Data were collected over a 1.0 mm length at a resolution of 0.056  $\mu\text{m}/\text{point}$ . Five single line scans at different locations were

collected and processed using a two-point leveling subtraction. The resultant arithmetic roughness ( $R_a$ ) values were calculated. Gloss measurements were collected according to ASTM D523 using a PCE Instruments PCE-PGM 100. The results are presented in Table 1.

Table 1. Coating characterization results.

Method	Parameter	SOA	BE
Sty Prof	$R_a$	$0.02 \pm 0.01 \mu\text{m}$	$0.02 + 0.01 \mu\text{m}$
Gloss Meter	$20^\circ$	72 AU	101 AU
	$60^\circ$	92 AU	105 AU
	$85^\circ$	100 AU	97 AU
Gon:	$\theta_A$	$87 \pm 1^\circ$	$81 \pm 6^\circ$
Water	$\theta_R$	$71 \pm 1^\circ$	$63 \pm 6^\circ$
Gon:	$\theta_A$	$71 \pm 1^\circ$	$65 \pm 3^\circ$
EG	$\theta_R$	$41 \pm 1^\circ$	$32 \pm 4^\circ$

**Durability Characterization.** Surface hardness and scratch resistance were determined using several techniques (Table 2). A Barcol impressor test was performed on the coated surfaces according to ASTM D2583. Both pencil hardness testing and a sclerometer (Elcometer 3092) were utilized to determine scratch resistance according to ASTM D3363 and G171, respectively. Pencil hardness values are reported as the softest pencil lead that scratched the surface.

Adhesion and cohesion properties of the coating were determined via cross-hatch testing and impact testing according to ASTM D3359 and D2794, respectively. Impact testing was performed using an Elcometer 1615 impact tester with a 1 kg drop weight and a 15.9 mm radius impact surface. Testing was conducted from drop heights of 40, 60, and 80 cm. Digital images of the results (units = kg cm) are shown in Fig. 2. The coatings were further evaluated via mandrel bend testing according to ASTM D522.

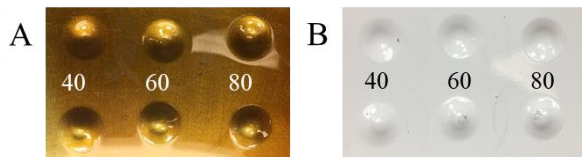


Figure 2. Impact panels of A) BE and B) SOA coatings.

Taber abrasion testing was conducted to simulate coating durability in the harsh, abrasive aircraft wing leading edge environment, according to ASTM D4060 using a Qualitest GT-7012-T and H-18 Taber wheels (Table 2). Tests were conducted using a custom sample support that utilized four  $\sim 3.73$  cm diameter samples centered on the abrasion wheel wear path. The coated surfaces were subjected to 1200 revolutions at 60 rpm.

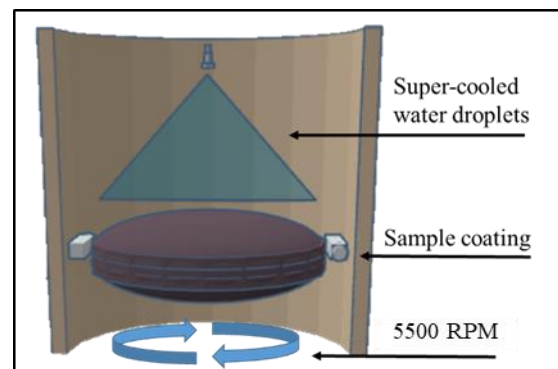
Table 2. Durability characterization results.

Method	Parameter	SOA	BE

Barcol	Hardness	$95 \pm 1$ B	$73 \pm 3$ B
Pencil hardness	Lead Hardness	H	F
Sclerometer	Hardness	0.3 N	0.4 N
Cross-hatch	Class	4B	5B
Mandrel Bend	Crack Length	None observed	None observed
Impact testing	Compression	80 kg cm	80 kg cm
	Tension	80 kg cm	80 kg cm
Taber abrasion	Wear Index	$62 \pm 3$	$27 \pm 1$

## Performance Characterization

**Ice Adhesion Strength (IAS) Characterization.** IAS was determined on a custom-built laboratory-scale ice adhesion testing device (AERTS Jr.) illustrated in Scheme 1.<sup>7</sup> Impact ice was accreted at test temperatures ranging from  $-16$  to  $-8^\circ\text{C}$  with a calculated liquid water content of  $0.30 \text{ g/m}^3$  and droplet mean volumetric diameter of  $20 \mu\text{m}$ . These conditions fall within the FAR Part 25/29 Appendix C icing envelope.<sup>1</sup> Both the coated sample disk and a control disk (highly roughened such that ice would detach from the test surface first) were weighed and mounted onto an Al rotor that was subsequently mounted in the refrigerated centrifuge in AERTS Jr. The rotor was spun up to approximately 5500 rpm (93 m/s) and thermally equilibrated at temperature for at least 20 min prior to testing. Supercooled microdroplets of water were introduced through a NASA MOD 2 nozzle (developed for the icing research tunnel at NASA Glenn Research Center) located above the plane of rotation. Ice release from the sample was detected by an accelerometer attached to a ballistic wall surrounding the centrifuge. The difference in accreted ice mass between the two disks was equated to the shed ice mass from the sample surface that was utilized to calculate IAS according to Equation 1 where  $m_{ice}$ ,  $v$ , and  $r$  are the mass of shed ice, linear velocity at the sample surface at the time of shed, and the rotor radius, respectively. For the work described here, the control surface was Alclad aluminum alloy 2024 T3.



Scheme 1. AERTS Jr located at NASA Langley

$$IAS = \frac{m_{ice} v^2}{r} \quad (\text{Eq. 1})$$

## Discussion

A balance of durability and performance must be considered for any coating formulation intended to be an external commercial aircraft coating. The work described here was undertaken to enable comparison of research formulations to established benchmarks across an array of general characterization, durability, and performance analytical techniques. Test standards and metrics derived from SOA exterior commercial aircraft coatings were utilized as a starting position for how to conduct the durability/performance evaluation. It is anticipated that additional analyses may be required to fully assess the applicability of a coating for a low ice adhesion application. Standards for low ice adhesion coatings for general aviation and unmanned aerial vehicles are likely to differ and the work described here may be considered as a starting point for establishing those criteria.

Surface property characterization results for the two coatings are shown in Table 1. Except for a slight variation in contact angle values, these two materials exhibited similar surface properties. This is particularly relevant for consideration of the durability and performance results, especially with respect to ice adhesion properties as roughness is known to play a significant role in ice adhesion strength.<sup>8</sup>

Results from the durability evaluation are summarized in Table 2. Three different hardness determination techniques were performed due to each of these approaches having an element of subjectivity. As can be seen, Barcol impression testing yielded a greater value for the SOA coating indicating that this coating may exhibit slightly lower compressibility. Pencil hardness results suggested the SOA was harder to scratch ( $H > F$ ) while the sclerometer results suggested that the BE coating was the harder of the two. However, these differences were minor suggesting the two were comparable. Impact testing was determined to be a particularly useful technique for assessing coating performance because it is rapid, the results are easy to interpret, and the success criteria are finite. Both coatings were determined to successfully pass this evaluation at the most demanding condition required, i.e., 80 cm drop height.

The most compelling results regarding durability evaluation were observed via Taber abrasion testing which is meant to simulate the harsh leading edge environment. Therefore, the abrading wheels used here were particularly abrasive. As can be seen in Table 2, the wear index for the BE coating was significantly lower than the SOA coating. This indicated that the BE coating would be anticipated to be more resilient in an abrasive environment than the SOA coating.

The primary method for determining coating performance in this work was measuring IAS using AERTS Jr. The results for this characterization are shown in Fig. 3. Due to the complexity of this measurement, an accepted data variability is  $\pm 20\%$ . As is the case for most materials, IAS value decreased upon increasing temperature for all surfaces discussed here. The significance between average

values was statistically evaluated via ANOVA and student t-test calculations. Based on these analyses, there was no statistical significance between any surface at  $-12$  or  $-16$  °C. However, both coated surfaces were determined to be statistically better than the Al clad surface at  $-8$  °C. The difference between average IAS values for the two coated surfaces was not statistically significant at this temperature.

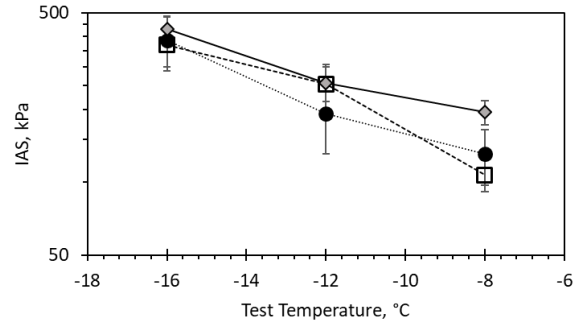


Figure 3. IAS values. Data points for the Alclad surface, BE, and SOA coatings are represented as gray-filled diamonds, unfilled squares, and filled circles, respectively. The dashed and solid lines are meant to guide the eye.

Although the durability and performance characterization was extensive, there are other techniques that could be utilized. For durability, additional testing to be performed includes solvent soaking in aircraft fluids, UV weathering, and thermal cycling. For performance, the length of time that a coating retains de-icing fluid, the hold over time, is of great importance. Although this property is not considered directly here, it is possible to utilize EG contact angle measurements to infer the wetting nature of de-icing fluid on a surface of interest. In this study, the two coatings were comparable.

## Summary

General characterization, durability, and performance analysis were performed on a SOA commercial aircraft coating and an epoxy formulation identified as a baseline from which to generate novel research coatings. The results of this analysis will be utilized as a benchmark for comparison of other potential low ice adhesion coating formulations. The BE coating demonstrated similar physical and durability properties to the SOA coating with the exception of Taber abrasion, where the BE exhibited a significant improvement in wear index.

## References

1. R.K. Jeck, Icing Design Envelopes (14 CFR Parts 25 and 29, Appendix C) Converted to a Distance-Based Format. Federal Aviation Administration, 2002, COT/FAA/AR-00/30.
2. X. Huang, et al., *Prog. Aerospace Sci.* **2019**, *105*, pp 74-97.
3. H. Sojoudi, et al., *Soft Matt.* **2016**, *12*, pp 1938-1963.
4. R.J. Varley, et al., *Prog. Org. Coat.* **2012**, *74*, pp 679-686.
5. C. Laforte, et al., Icephobic Coating Evaluation for Aerospace Applications. In *AIAA SciTech Forum*, National Harobr, MD, 2014.
6. J. Soltis, et al., *AIAA Journal* **2015**, *53*, pp 1825-1835.

7. J.G. Smith Jr, et al., Design and Development of a Laboratory-scale Ice Adhesion Testing Device. In *41st Annual Meeting of The Adhesion Society*, San Diego, CA, 2018.
8. M. Susoff, et al., *Appl. Surf. Sci.* **2013**, 282, pp 870-879.